SEARCH FOR RESONANT DOUBLE HIGGS PRODUCTION WITH bbZZ DECAYS IN THE $b\bar{b}\ell\ell\nu\bar{\nu}$ FINAL STATE IN pp COLLISIONS AT $\sqrt{s} = 13$ TeV

by

Rami Kamalieddin

A DISSERTATION

Presented to the Faculty of

The Graduate College at the University of Nebraska

In Partial Fulfilment of Requirements

For the Degree of Doctor of Philosophy

Major: Physics and Astronomy

Under the Supervision of Professor Ilya Kravchenko

Lincoln, Nebraska

May, 2019

SEARCH FOR RESONANT DOUBLE HIGGS PRODUCTION WITH bbZZ DECAYS IN THE $b\bar{b}\ell\ell\nu\bar{\nu}$ FINAL STATE IN pp COLLISIONS AT $\sqrt{s} = 13$ TeV

Rami Kamalieddin, Ph.D.

University of Nebraska, 2019

Adviser: Ilya Kravchenko

Since the discovery of the Higgs boson in 2012 by the ATLAS and CMS experiments, most of the quantum mechanical properties that describe the long-awaited Higgs boson have been measured. Due to the outstanding work of the LHC, over a hundred of fb^{-1} of data have been delivered to both experiments. Finally, it became sensible for analyses teams to start working with a very low cross section processes, which made it possible to observe rare decay modes of the Higgs boson, e.g., a recent success in observing ttH and VHbb processes. One of the main remaining untouched topics is a double Higgs boson production. However, additional hundred of fb^{-1} per year from the HL-LHC will not necessarily help us much with the SM double Higgs physics, the process may remain unseen even in the most optimistic scenarios. The solution is to work in parallel on new reconstruction and signal extraction methods as well as new analysis techniques to improve the sensitivity of measurements. This thesis is about both approaches: we have used the largest available dataset at the time the analysis has been performed and developed/used the most novel analysis methods. One of such methods is the new electron identification algorithm that we have developed at the CMS electron identification group, to which I have had a privilege to contribute during several years of my stay at CERN.

The majority of this thesis is devoted to techniques for the first search at the LHC for the double Higgs boson production mediated by a heavy narrow-width resonance

in the $b\bar{b}ZZ$ channel: $X \to HH \to b\bar{b}ZZ^* \to b\bar{b}\ell\ell\nu\bar{\nu}$. The measurement searches for a resonant production of a Higgs boson pair in the range of masses of the resonant parent particle from 250 to 1000 GeV using 35.9 fb^{-1} of data taken in 2016 at 13 TeV. Two spin scenarios of the resonance are considered: spin 0 and spin 2. In the absence of the evidence of the resonant double Higgs boson production from the previous searches, we proceed with setting the upper confidence limits.

"... a place for a smart quote"

Lenin, 1922.

ACKNOWLEDGMENTS

This will be a long list!

Table of Contents

List of Figures

List of Tables

Chapter *1*

Physics Object Reconstruction

Excellent spatial resolution of the CMS trackers, high granularity of the calorimeters, and almost 4π coverage of the detector, allowed the CMS to introduce the particle flow (PF) algorithm [**?**] for a global event reconstruction. PF takes the input from all subdetectors, analyses the redundant information, removes the duplicate one, and forms the physics objects. PF procedure starts with identification of tracks and calorimeter clusters, then the reconstruction of the physics objects is performed, such as electrons, muons, jets, etc. In this section we will discuss the whole PF approach and all key elements of this reconstruction sequence.

1.1 Track Reconstruction

The reconstruction starts with the clusters of signals ("hits") in the inner tracker. The information from these clusters in the Pixel and Strip subdetectors is aggregated based on their signal-to-noise ratios. The charge-weighted averaging is performed (for different particle charge hypothesis), as well as other corrections are further applied to identify the real hit positions.

The helix trajectory that the particle follows in the magnetic field inside of the detector is characterised by five parameters: the direction in η, the 3D position with respect to the reference point, which is the centre of the IP, and the curvature of the track with

the radius R. This information is enough to compute estimates of basic physics quantities, however, the this task is complicated by the presence of event high multiplicity (number of charged particles produced in the same event) and also by the physics aspect of the electron propagation in matter: an electron traversing the detector has nearly 85 % probability to emit a bremsstrahlung photon. Hadronic effects also need to be taken into account: a hadron has a 20 % probability to experience multiple scattering on the nuclei of the detector before reaching the HCAL.

To keep the track finding efficiency high, while maintaining low the efficiency of miss-identified tracks, track reconstruction is performed sequentially using the combinatorial track finder (CTF) [**?**]. First the "purest" tracks are reconstructed, they have high p_T and the hits point towards the primary vertex (PV). The term PV is used to refer to the vertex which is the actual point of origin of the produced particle, when several other hard scattering vertices are present in the event. Then these pure tracks are removed from the collection of tracks and another round of the track reconstruction starts. This procedure applied several times reduces the combinatorial factor and also simplifies the identification of tracks with the low p_T or those which do not point to the PV. During each iteration, the reconstruction follows these steps:

- Seed generation. Rough estimates of the particle trajectories ("seeds") are produced using either three hits or two hits and a PV constraint. Based on which iteration the algorithm is at, some additional constraints are applied, e.g., a minimal p_T requirement, the need for the seed to originate close to the beam spot, etc.

- Trajectory building. Initial seeds are projected towards the compatible hits in the next layers based on the Kalman Filter (KF) procedure [**?**]. The extrapolation is done until the outermost layer of the tracker is reached or when a "terminating condition" is satisfied, e.g., when the iteration accumulated the maximum number of invalid hits ("fake hits"). Each obtained trajectory is updated using a KF approach based on the compatibility of hits to form a better track candidate. The procedure is complicated

by the fact that the same initial seed can give rise to several track candidates or vice versa, the same track candidate may be compatible with different seeds. Additionally, the trajectory building step should take into account energy loses of the particle due to multiple scattering on the detector material, inhomogeneities of the tracker material, and the effects of the regions of non constant magnetic field.

- Track fitting. After the track candidate has been built, the track parameters are refitted by a KF and the "smoother". This step uses the full available information about the track and gives optimal estimates of the track parameters. To remove a large number of fake tracks, which are present due to a very complicated nature of the problem and the high track multiplicity in the event, a multivariate (MVA) selection is applied. MVA incorporates variables that discriminate real tracks from the fakes: the signed transverse curvature and impact parameters (with respect to the beam spot), the polar and azimuthal angles, number of missing hits, the fit quality variables, etc.

The CTF procedure runs for 10 iterations. For 2016 collisions with a mean pileup (additional hard scattering vertices) of 24, the CTF efficiency to identify real tracks varied from 80 to 95% with the mis-identification efficiency of 5 - 10 %.

1.1.1 Muon tracking

Muons are detected by the inner tracker and also by the outer (muon) tracker. This greatly improves muon track reconstruction and motivated the development of a dedicated muon reconstruction algorithms. The ninth and the tenth iterations of the CTF are focused on the muon reconstruction. These iterations are using three separate algorithms to identify:

- Standalone muons. This algorithms uses only muon tracker information: DTs, CSCs, RPCs. Hits from the inner chambers are used as seeds and projected to hits in the

outer chambers. Then, a standard KF procedure is used to identify track candidates, which are called standalone muons.

- Tracker muons. Only the inner tracking information is used to form tracks. Tracks are further projected to muon subsystems, where a compatibility with at least one muon hit is required. This algorithm works with low momentum muons: tracks with p_T above 0.5 GeV and a total momentum greater than 2.5 GeV.

- Global muons. Tracker tracks and standalone tracks are projected to the outermost layer of the muon system, checking the compatibility between two approaches. The resulting combined set of track hits is refitted to produce a global muon track. Mostly high momentum muons with $p_T >$?? 200 GeV profit from this algorithm.

1.1.2 Electron tracking

Electrons are also detected by the inner tracker, however, their reconstruction is complicated by the fact that they emit bremsstrahlung photons and the trajectory becomes more complex. As a result, the clustering algorithms need also to identify the bremsstrahlung photons and account for the fact that the energy clusters corresponding to these photons may be located outside of the main electron trajectory, when extrapolated to the ECAL.

Since a KF approach assumes that energy losses are Gaussian, and this is not the case for electrons, a dedicated procedure is developed - a modified KF - the Gaussian Sum Filter (GSF) [144]. In this method the radiated energy losses are approximated by the sum of Gaussian distributions.

The electron seeds for the GSF are built using the ECAL information. Two different approaches are developed for the track reconstruction:

- Super Cluster based electrons. Cluster of energy in the ECAL and grouped together to form super clusters (SCs). Using the information of the energy spread among the

clusters, the curvature of the electrons is estimated and tracker seeds are formed, with the SC position as a constraint.

- Tracks based electrons. Tracks from the inner tracker are projected to ECAL clusters, checking the compatibility using quality variables, such as χ^2, number of missing hits (absent hits along the path of the track), etc.

A typical momentum resolution for electrons in $Z \to e^- e^+$ decays is approximately 1.7 - 4.5%.

1.1.3 Primary Vertex reconstruction

At the LHC energies, several hard scattering vertices are produced in each collision. The location of all primary vertices (PV) is reconstructed using the tracks. However, normally only one (the main PV) out of these vertices (referred to as additional vertices or pileup) produces the interesting physics interactions. All the vertices are important since they are reused in the feed-back loop of the track reconstruction procedure. Also, a precise identification of primary vertices is important for determining the effect of the pileup on all physics objects in general and b-tagging in particular (will be discussed later in this chapter).

The PV identification consists of three steps: the tracks are selected, then the tracks from the same PV are combined in clusters, and, finally, the position of the PV is determined from the fits to tracks.

Selecting the tracks, only those consistent with the location of the PV are considered. Several variables are used to improve the quality of the track selection procedure: the transverse impact parameter (the relative distance in the vertical plane with respect to the centre of the beam spot), the number of strip and pixel hits associated with a track, and the χ^2 of the fit .

Clustering of the tracks is based on their z position with respect to the beam spot. A deterministic annealing (DA) algorithm [**?**] is used to find the global minimum for this problem with many degrees of freedom. The idea of this algorithm is based on the physics example of a system approaching a state of minimal energy through a series of temperature reductions.

Once the clustering is completed and PVs are identified, the candidates with more than two tracks are fitted using an adaptive vertex fitter [**?**]. The result of this procedure is a set of probabilities assigned to tracks. This can be thought of as a likelihood that the track originated from the given vertex.

The resolution of PVs varies between 10 - 100 μm to 100 ?m and depends on track qualities. The main PV is determined as the vertex with the highest sum of the squared p_T.

1.1.4 Particle Flow links and blocks

Usually a particle leaves the signal in several CMS dubdetectors which is stored as PF [**?**] elements. To connect these PF elements, the link algorithm (LA) was developed. The LA can test any pair of elements in the event. To speed up the calculations, only pairs of elements that are "neighbours" in the specified $\eta - \varphi$ plane are considered. When the pair of elements is linked, the LA determines the distance between the elements which is related to the quality of the link. This procedure produces PF blocks of elements, which are connected either by a direct or an indirect link (through the common elements)

The procedure produces inner tracker-calorimeter, HCAL-ECAL cluster-to-cluster, ECAl-ECAL, and ECAL-Preshower links. In most cases the link distance is defined as the $\eta - \varphi$ or $x - y$ distance between the two cluster positions. In case of the ambiguity when, e.g., several HCAL clusters are linked to the same ECAL cluster, only one link is kept - with the smallest distance.

The last stage of the link algorithm is dedicated to formation the inner tracker-muon

system links. Once all links are established and PF blocks are formed, the PF algorithm proceeds reconstructing objects in the following sequence: muon candidates (with corresponding PF tracks and clusters been removed from the PF block), electron candidates (taking into account bremsstrahlung photons) and high momentum isolated photons (with related tracks and clusters also been removed), and, finally, charged hadrons and non-isolated photons.

The elements that are still left in the PF blocks are then re-considered for another round of identification of: charged hadrons and neutral hadrons, photons from parton fragmentation and hadronization, and jet decays. Lastly, when all PF blocks have been sorted out, the global event description is completed and the reconstructed event is re-processed by a post-processing step (PP step), which addresses the possible particle misidentification and misreconstruction during the previous steps.

1.1.5 Muons

Muon reconstruction is the first stage of the PF algorithm. It identifies muons using global and inner tracker muon properties. Global muon candidates are selected at this step and the isolation requirement (explained later in this chapter) is applied. This isolation requirement is efficient enough to reject hadrons mis-identified as muons.

The muons inside jets or secondary muons from hadron decays are complicating the identification of prompt muons, such as those originating from Higgs, W, or Z boson decays. Therefore, additional more stringent selection is further applied.

For non-isolated global muons, in addition to the Tight WP selection, it is required to have more than two matching track segments in the muon detectors or that the calorimeter energy deposits are compatible with the muon candidate. This selection discriminates against the high p_T hadrons.

If muons fail Tight WP, there are still several "recovery" iterative procedures that use the relax the selection criteria.

However, even at this stage the muon identification and reconstruction is not finished. Charged hadrons reconstructed during the next PF stages can be reconsidered as muon candidates. Only after the whole PF sequence is completed, including the PP step, the PF algorithm terminates.

All muons considered for this measurement are global muons that satisfy the Tight WP requirements (Tight WP as an initial selection) with extra requirements on the number of hits in the tracker and muon system, on the impact parameter, and the quality of the global track.

The efficiency ϵ to successfully identify a prompt isolated lepton (in our case muon or electron) can be decomposed as:

$\epsilon = \epsilon_{tracker} \cdot \epsilon_{ID|tracker} \cdot \epsilon_{ISO|ID}$

where the first term refers to the tracker efficiency, the next term is the Bayesian term which refers to the identification (ID) efficiency given that the lepton already passed the tracker requirements, and the final term refers to the isolation (ISO) efficiency given that the lepton already satisfied identification criteria. All the efficiencies are well optimised in the CMS and are in the range from 85 to more than 99 % depending on the p_T and η of the lepton (muon in this case).

The muon resolution for 20 to 100 GeV momentum range varies from 1 % in barrel to 5 % in endcaps.

1.1.6 Electrons and isolated photons

The reconstruction of electrons is complicated by the fact that they lose energy emitting bremsstrahlung photons and, thus, their trajectory becomes more complex than the one of muons. Additionally, bremsstrahlung photons often convert to e^+e^- pairs. And this is a recursive process: daughter electrons also emit photons. Due to this complication, the procedure to reconstruct electrons and photons is similar. First a GSF track plays a role of the seed for the electron candidate. An ECAL SC with no links to the GSF track is used as

a seed for the photon candidate. For both electron and photon candidates energy deposits in the HCAL must not exceed 10% of the ECAL energy.

Then all ECAL clusters in the PF block are linked to the SC or to one of the GSF track tangents of the candidate. The total energy of the collected ECAL clusters is corrected for the energy losses during the linking procedure and is assigned to photons. The electron candidate is formed from a combination of the corrected ECAL energy and the electron direction given by the GSF track. Additional MVA discriminator of O(20) variables is applied to improve electron identification efficiency. The MVA approach based on the Boosted Decision Trees (BDT) classifier [**?**] profits from the following highly discriminating variables: the amount of energy radiated off the GSF track, the distances between the ECAL SC position and the projection from the GSF track, track-cluster linking variables, KF and GSF track quality variables, etc.

Photon candidates are kept if photons are isolated and the corresponding configuration of ECAL energy deposits is compatible with those expected from a given photon shower.

All identified electron and photon tracks and clusters in the PF block are masked before the algorithm starts processing hadrons. Since some offline physics analyses may apply different selection for electrons and photons, PF selection is relatively loose and the full electron and photon reconstruction information is saved in case a different re-interpretation must be run. This allows to save time in the future since would not require running the complete PF algorithm again.

1.1.7 Hadrons and non-isolated photons

After the muons, electrons, and isolated photons get reconstructed, they are removed from the PF blocks. The next PF algorithm iterations proceed with hadrons from jet fragmentation and hadronization. These particles can be seen by the detector as charged pions, kaons or protons, neutral pions and kaons, and non-isolated photons from neutral pion decays. During the reconstruction, the precedence is given in the ECAL to photons over neutral

hadrons. This priority does not hold above $|\eta| > 2.5$. In that region ECAL clusters linked to a given HCAL cluster are identified as hadrons and, only if ECAL clusters are without such a link, then they are classified as photons.

What is left in the PF block, gets classified in the following manner: if energy deposits are consistent with the energy hypothesis from the tracker, then no neutral hadron is found and each track that remains - corresponds to a charged pion candidate.

In situations when the energy deposits in the ECAL does not match well the energy hypothesis from the tracker and this discrepancy is larger than three standard deviations, a new muon reconstruction starts, with the relaxed muon selection. This approach allows to improve the muon identification efficiency without increasing the mis-identifiedmuon rate.

If the track momentum sum is still significantly larger than the calorimetric energy,the excess in momentum is often found to arise from residual misreconstructed tracks with ap-Tuncertainty in excess of 1 GeV. These tracks are sorted in decreasing order of theirpTuncertainty and are sequentially masked either until no such tracks remain in the PF block or until

The hadron traversing the material of the tracker interacts with the nuclei of the tracker and often produces secondary hadrons. These hadrons evidently are produced outside of the PV - at the secondary (intermediate) interaction vertex. When the charged-particle tracks corresponding to these secondary particles are linked together, the resulting secondary particle candidates can be replaced in the list of reconstructed particles by a single (original) charged hadron.

Estimate of the energy of the primary charged hadron is then given by:

$E = E_{secondary} + f \cdot p_{primary}$

where $E_{secondary}$ is a vectorial sum of the momenta of the secondary charged particles, $p_{primary}$ is the momentum of the incoming track, and f is the factor determined from the simulations.

1.1.8 Jets and jet corrections

Jets are collimated streams of particles created in the fragmentation and hadronization process of the original parton, quark or gluon. As jets propagate through the CMS detector, they leave tracks in the tracking system and interaction showers in the calorimeter crystals.

Several jet reconstruction algorithms have been developed. In the Higgs boson group of the CMS, most measurements are using $anti - k_T$ algorithm [**?**]. If the jet clustering uses PF particles - PF jets are reconstructed. If only the ECAL and HCAL information is used - calorimeter jets are identified ("calo jets"). When all stable particles (in case of the simulation, at the generator level) excluding neutrinos are used - reference jets are reconstructed ("Ref jets"). In this measurement PF $anti - k_T$ jets are used.

The anti$-k_T$ algorithm is one of the cone algorithms that takes as input a collection of PF objects inside of the cone of the radius R (usually defined by the jet size). The algorithm defines the distance parameter: $d_{ij} = \min(\frac{1}{p^2_{T_i}}, \frac{1}{p^2_{T_j}}) \times \frac{R^2_{ij}}{R}$,
where p_{T_i} and p_{T_j} refer to the transverse momenta of PF particles i and j, R_{ij} is the distance in the $\eta - \varphi$ plane.

An additional d_{iB} parameter is defined as the distance between the particle i and the beam axis: $d_{iB} = \frac{1}{p^2_{Ti}}$.

The algorithm iteratively finds the minimum distance choosing at each step the minimal value in the (d_{ij}, d_{iB}) pair, using a collection of the PF particles as an input.

If the minimum distance is d_{ij}, then the four-vectors of i and j particles are summed to form a new particle. Particles i and j are removed from the initial input collection. If the minimum distance is d_{iB}, then the particle i is considered a jet. This particle is also removed from the set of particles and the algorithm continues until all initial particles have been combined into jets. The mechanics of the algorithm clusters soft candidates with the hardest particles first, producing a perfect cone-shaped jets.

PF jets are used in this thesis over Calo jets since the former have a superior angular resolution. PF algorithm allows the precise determination of the charged hadron direction

and momentum, while in calorimeters, the energy deposits of charged hadrons are spread along the φ direction in the presence of the magnetic field. This gives an extra degradation of the azimuthal angular resolution of jets.

On average, the jet energy is formed by: 65% by charged hadrons, 25% by photons, and 10% by neutral hadrons. The possibility to identify the contributors to the total jet energy during the jet reconstruction is one of the reasons to use the PF algorithm for jet reconstruction. In practice the identification of particles inside jets is done comparing the jet energy fractions measured in PF jets to those of the corresponding Ref jets.

To remove the jet energy dependence on p_T and η of the jet and, hence, to "flatten" the corresponding two dimensional map, the jet energy correction (JEC) procedure is introduced. Additionally, the jet energy resolution (JER) correction is necessary. The latter is defined as the Gaussian width of the ratio of the energies of the corrected PF jets to Ref jets. Both corrections improve the angular resolution, energy response, and energy resolution of jets.

JEC scales the four-momentum of jets. The various detector effects are addressed. Depending on how sensitive the physics analysis is to this correction type, one can factorise this correction into separate components and apply them individually in a sequence. Most important individual corrections remove: energy contributions due to pileup, effects of the calorimeter response, residual Data-MC discrepancies, effects of the jet flavor, etc.

JER smears the four-momenta of reconstructed jets to match the energy resolution observed in data. The smearing procedure derives the correction factors which scale the reconstructed jet momentum with respect to the the same jet clustered from the generator MC level.

1.1.9 The b tagging and secondary vertices

In this measurement one of the Higgs bosons decays to b quarks. Jets produced during the hadronisation of b quarks are called b jets. A dedicated b tagging is necessary since Higgs

boson decay to b quarks has the highest branching fraction of almost 58% and is a great test of the SM validity.

B quarks will produce jets that contain B mesons, which have a relatively long lifetime $c\tau \approx 500\mu$ m. This distance travelled at almost the light speed would correspond to a dislocation of a few mm from the PV. The new positions where the B meson decays, will be clearly seen in the detector. This displaced vertex, the secondary vertex (SV), is a unique signature of b quarks and is used to identify their decays. Sometimes the vertex cannot be unambiguously reconstructed, but even in these cases the properties of tracks within b jets are different from the ones originating from gluons or light quarks (light jets).

After passing the selection criteria, tracks are considered for b tagging. The selection requirements, that include kinematic and impact parameter properties of tracks, are needed to reject fake tracks, tracks coming from pileup vertices, and tracks from the long-lived hadrons.

Two main approaches are used to reconstruct the secondary vertices (SV). One of the methods that pioneered the b tagging is an adaptive vertex reconstruction (AVR) algorithm. AVR is based on the adaptive vertex fitter, it uses the tracks associated with jets and finds PVs and SVs. The other algorithm is the inclusive vertex finder (IVF). IVF uses all the tracks in the event and is implemented with the selection looser than for the AVR.

As for the b tagging itself [**?**, **?**], multiple algorithms (taggers) have been developed and successfully used over the last decade. The most known ones are:

- the jet probability (JP) and the jet b probability (JBP) tagger. Both are based on the probability of a jet candidate to be compatible with the PV using impact parameter significance (IPS) variables.

- The soft electron tagger (SET) and soft muon tagger (SMT). These taggers are based on the presence of soft leptons within jets. It focuses on leptonic decays of B hadrons.

- The combined secondary vertex (CSVv2) tagger. This is a more complex tagger based

on the MVA technique. It uses displaced tracks and secondary vertices to tag b jets and takes as input IPS, decay length, SV parapeters, number of SVs, etc. This tagger can use both AVR and IVF vertices.

In this physics analysis a new MVA based (cMVAv2) tagger was used. This superior tagger uses the outputs from all the aforementioned "fundamental" taggers: JP and JBP, SET and SMT, CSVv2 using both AVR and IVF vertices. These ensemble learning procedure [**?**], that combines outputs from fundamental taggers into one complex MVA based tagger that produces the final output, is a popular machine learning technique that has been proven to lead to better results than the ones achieved by individual algorithms separately.

1.1.10 Missing transverse momentum

When neutrinos are present in the event, they cannot be directly detected by the CMS, specific neutrino detectors would be needed in this case. However, using the CMS detector one can indirectly estimate the momentum of neutrinos. This procedure relies on the methods of the missing transverse momentum $\not{p}_{\mathrm{T}}$ (or missing transverse energy $\not{E}_{\mathrm{T}}$ (MET)).

MET is constructed using all PF particles in the event and is calculated as:

$\not{p}_{\mathrm{T}} = \vec{p}_T^{\,miss} = |-\sum_i^N \vec{p_{Ti}}|$.

To reconstruct $\not{p}_{\mathrm{T}}$, the CMS relies on almost 4π coverage of the detector and precise measurement of the particle properties using PF algorithm that takes information from all subsystems. Produced $\not{p}_{\mathrm{T}}$ is still considered "raw", since is not JEC and JES corrected. After these corrections are applied, one obtains $\not{p}_{\mathrm{T}}$ that is called "Type-1 corrected MET". This is the definition of MET that is recommended by the CMS JetMET particle Object Group (POG) group and is used in this measurement. Additional set of filters and corrections is further applied to reject events with artificially large $\not{p}_{\mathrm{T}}$ due to the presence of several noise sources, such as ECAL dead cells, poor quantity muon candidates, HCAL noise.

1.1.11 Lepton isolation

As mentioned before, lepton isolation is a great method to remove clear fakes and select real prompt muons and electrons produced by Higgs boson decay or by the weak decays of Z or W bosons. The isolation quantifies the activity of other particles around the particle of interest. The lepton isolation is defined as the scalar sum of the p_T's of all charged and neutral hadrons and photons inside a cone of the radius $\Delta R < 0.3 - 0.4$(depending on the working point (WP)). The sum is normalised by the p_T of the lepton of interest:

$I_{PF} = \frac{1}{p_T}(\sum^{\gamma} p_T^{\gamma} + \sum^{h^{\pm}} p_T^{h^{\pm}} + \sum^{h^0} p_T^{h^0})$

1.1.12 Pileup interactions

Pileup interactions which have produced charged hadrons reconstructed as tracks can be identified as additional primary vertices (see Sec. 2.3.1). These hadrons can therefore be flagged as pileup and removed from the list of candidates in the event. This procedure is dubbed charged-hadron subtraction (CHS), and it should be understood that the reconstruction algorithms described in previous sections are based on CHS-cleaned candidate collections (PF+CHS) [188]. For neutral hadrons, photons, and charged hadrons beyond tracker acceptance or not removed by CHS, no such straightforward procedure is possible. In one strategy pursued, the average pT density due to pileup is estimated, relying on the uniformity of pileup energy deposits. This density, ?, can then be multiplied by the ?area? A of a candidate, and the result ? ů A subtracted from the candidate?s pT. For jets, A is taken to be their catchment area [203,204]. The effective area Aeff used to correct the electron isolation [194] 2 is directly related to the area of the isolation cone, (?R) , and their (absolute) isolation is then given by

PF ?? p +max?0, p + p ??A ?, (2.12.) T ? T T eff? ś?0i??? i?h i?h ?? e,abs. ??i ????i ??i ?? ś0 where the sums run over all PF charged CHS (h) and neutral (h , ?) candidates within a cone of ?R ?? 0.3 around the electron. An alternative method, used to correct muon isolation, is based on the observed ratio of ?? ? 0.5 between neutral and charged

pileup energy. The contribution to the isolation due to neutral pileup can therefore be estimated locally from the measured charged pileup energy in the isolation cone: ?,abs. ?? i ?? ?? i ?? i ?? i?? Iso ?? p +max?0, p + p ??? p ? (2.13.) PF T ? T T T? ś?0i??ś? i ? h i ? h i ? PU h ?? Here the sums run over the same collections as in (2.12), in a cone of ?R ?? 0.4 around the muon. In the last term of (2.13), only charged hadrons associated with pileup vertices are considered. miss The calibration of the pT is not expected to be affected by pileup, since pileup miss interactions produce little to no true pT . However, its resolution can be significantly miss degraded due to the extra energy in the events. In addition to computing the p??T using CHS-cleaned candidates, a correction for the effect of neutral energy deposits, referred to as Type-0 correction, is applied. This correction is computed from the observed charged pileup candidates, assuming that for pileup the true charged and neutral total transverse momenta are exactly balanced, and that the charged candidates are perfectly measured.

Pileup particles give rise to additional deposits in the calorimeters, approximately uniformly distributed throughout the detector, that degrade the energy miss resolution of jets and of the pT . Extra hits from charged pileup particles in the trackers render track reconstruction more difficult due to the increased combinatorial background, resulting in a lower tracking efficiency and higher fake rate. As a consequence, but also due to the additional reconstructed tracks in the event, tasks such as b tagging become more challenging as well. Finally, the extra energy due to pileup impacts the estimate of lepton isolation, resulting in lower muon and electron selection efficiencies for a given isolation requirement. This sections describes the methods used to mitigate these effects

- somewhere a section on physics objects where you discuss that there are tracks, there are jets, there are b-jets, what it means an isolated lepton, what it means missing momentum, and so forth. For example, Ekaterina has a section on particle flow, if I remember right, where she discusses that. Or you can have a section that just discuses the proton-proton collisions environment and explains that many particles created in collisions are unstable

and decay right away. What is observable in an experiment such as CMS is longer-lived or stable particles. These include electrons, muons, photons, and some ground state hadrons. At the same time, energetic quarks or gluons hadronize and can be seen in a particle detectors as jets of hadrons (so define jets here). Same for tau leptons, we detect them either as electrons/muons, or hadronic jets. Etc. If you have such a conceptual paragraph here, some time later you can have a particle flow discussion when it is time to be more specific. But discussion at this level above would allow you to then discuss the requirements on CMS design using terms like b-jets or isolated leptons.

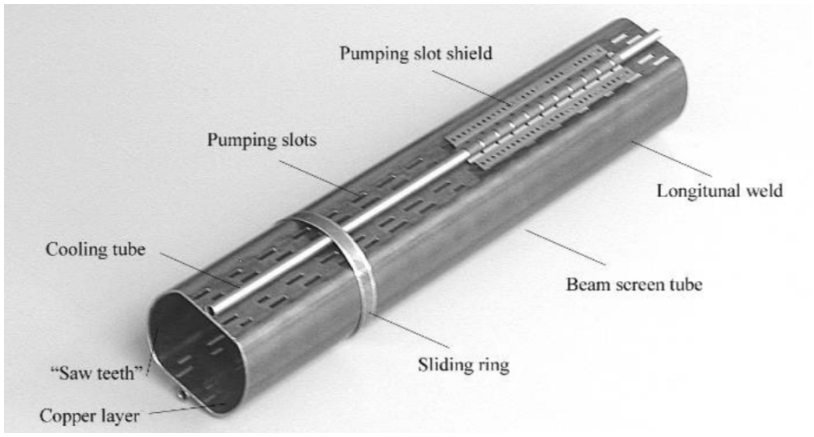

Figure 1.1: Beam screen.

EGAMMA AT LEAST SAY THAT HAS BEEN WORKING AND SHOW SOME PLOTS?

References

[1] Erwin Schrödinger. *Statistical thermodynamics; 2nd ed.* Cambridge Univ. Press, Cambridge, 1952.

[2] Richard Phillips Feynman, Robert Benjamin Leighton, and Matthew Sands. *The Feynman lectures on physics; New millennium ed.* Basic Books, New York, NY, 2010. Originally published 1963-1965.

[3] David J Griffiths. *Introduction to elementary particles; 2nd rev. version.* Physics textbook. Wiley, New York, NY, 2008.

[4] E A Davis and Isabel Falconer. *J.J. Thompson and the discovery of the electron.* Taylor and Francis, Hoboken, NJ, 2002.

[5] Oreste Piccioni. *The Discovery of the Muon*, pages 143–162. Springer US, Boston, MA, 1996.

[6] Carl Bender. Mathematical physics.

[7] G. Danby, J-M. Gaillard, K. Goulianos, L. M. Lederman, N. Mistry, M. Schwartz, and J. Steinberger. Observation of high-energy neutrino reactions and the existence of two kinds of neutrinos. *Phys. Rev. Lett.*, 9:36–44, Jul 1962.

[8] M. L. Perl, G. S. Abrams, and et al Boyarski. Evidence for anomalous lepton production in $e^+ - e^-$ annihilation. *Phys. Rev. Lett.*, 35:1489–1492, Dec 1975.

[9] K. Kodama et al. Observation of tau neutrino interactions. *Phys. Lett.*, B504:218–224, 2001.

[10] Eric W. Weisstein. Fundamental forces.

[11] S Chandrasekhar. *Newton's principia for the common reader*. Oxford Univ., Oxford, 2003. The book can be consulted by contacting: PH-AID: Wallet, Lionel.

[12] Charles W. Misner, Kip S. Thorne, and John Archibald Wheeler. *Gravitation / Charles W. Misner, Kip S. Thorne, John Archibald Wheeler*. W. H. Freeman San Francisco, 1973.

[13] Hanoch Gutfreund and Jurgen Renn. *The road to relativity: the history and meaning of Einstein's "The foundation of general relativity" : featuring the original manuscript of Einstein's masterpiece*. Princeton University Press, Princeton, NJ, Apr 2015.

[14] J. Butterworth. *Smashing Physics*. Headline Publishing Group, 2014.

[15] W N Cottingham and D A Greenwood. *An Introduction to the Standard Model of Particle Physics; 2nd ed.* Cambridge Univ. Press, Cambridge, 2007.

[16] C. Patrignani et al. Review of Particle Physics. *Chin. Phys.*, C40(10):100001, 2016.

[17] Andrew Wayne. QED and the Men Who Made It: Dyson, Feynman, Schwinger, and Tomonaga by Silvan S. Schweber. *The British Journal for the Philosophy of Science*, 46(4):624–627, 1995.

[18] Michelangelo L Mangano. Introduction to QCD. (CERN-OPEN-2000-255), 1999.

[19] R. P. Feynman. The theory of positrons. *Phys. Rev.*, 76:749–759, Sep 1949.

[20] Matt Strassler. Of particular significance: Conversations about science with theoretical physicist matt strassler.

[21] S. L. Glashow. Partial Symmetries of Weak Interactions. *Nucl. Phys.*, 22:579–588, 1961.

[22] F. Englert and R. Brout. Broken symmetry and the mass of gauge vector mesons. *Phys. Rev. Lett.*, 13:321–323, Aug 1964.

[23] Peter W. Higgs. Broken symmetries and the masses of gauge bosons. *Phys. Rev. Lett.*, 13:508–509, Oct 1964.

[24] G. S. Guralnik, C. R. Hagen, and T. W. B. Kibble. Global conservation laws and massless particles. *Phys. Rev. Lett.*, 13:585–587, Nov 1964.

[25] Pauline Gagnon. *Who cares about particle physics? : making sense of the Higgs boson, the Large Hadron Collider and CERN*. Oxford University Press, 2016.

[26] Precise determination of the mass of the Higgs boson and studies of the compatibility of its couplings with the standard model. Technical Report CMS-PAS-HIG-14-009, CERN, Geneva, 2014.

[27] Jennifer Ouellette. Einstein's quest for a unified theory. *APS*, 2015.

[28] S. M. Bilenky. Neutrino in Standard Model and beyond. *Phys. Part. Nucl.*, 46(4):475–496, 2015.

[29] Matthias U. Mozer. Electroweak Physics at the LHC. *Springer Tracts Mod. Phys.*, 267:1–115, 2016.

[30] Gennadi Sardanashvily. *Noether's theorems: applications in mechanics and field theory.* Atlantis studies in variational geometry. Springer, Paris, 2016.

[31] Steven Weinberg. The Making of the Standard Model. *Eur. Phys. J. C*, 34(hep-ph/0401010):5–13. 21 p. ; streaming video, 2003.

[32] Roger Wolf. *The Higgs Boson Discovery at the Large Hadron Collider*, volume 264. Springer, 2015.

[33] Jose Andres Monroy Montanez, Kenneth Bloom, and Aaron Dominguez. Search for production of a Higgs boson and a single Top quark in multilepton final states in pp collisions at $\sqrt{s} = 13$ TeV, Jul 2018. Presented 23 Jul 2018.

[34] Peisi Huang, Aniket Joglekar, Min Li, and Carlos E. M. Wagner. Corrections to di-Higgs boson production with light stops and modified Higgs couplings. *Phys. Rev.*, D97(7):075001, 2018.

[35] Matthew J. Dolan, Christoph Englert, and Michael Spannowsky. New Physics in LHC Higgs boson pair production. *Phys. Rev.*, D87(5):055002, 2013.

[36] Shinya Kanemura, Kunio Kaneta, Naoki Machida, Shinya Odori, and Tetsuo Shindou. Single and double production of the Higgs boson at hadron and lepton colliders in minimal composite Higgs models. *Phys. Rev.*, D94(1):015028, 2016.

[37] Albert M Sirunyan et al. Search for Higgs boson pair production in the $\gamma\gamma b\bar{b}$ final state in pp collisions at $\sqrt{s} = 13$ TeV. 2018.

[38] Alexandra Oliveira. Gravity particles from Warped Extra Dimensions, predictions for LHC. 2014.

[39] Lisa Randall and Raman Sundrum. A Large mass hierarchy from a small extra dimension. *Phys. Rev. Lett.*, 83:3370–3373, 1999.

[40] Alexandra Oliveira. Gravity particles from Warped Extra Dimensions, predictions for LHC. 2014.

[41] Kunihito Uzawa, Yoshiyuki Morisawa, and Shinji Mukohyama. Excitation of Kaluza-Klein gravitational mode. *Phys. Rev.*, D62:064011, 2000.

[42] H. Davoudiasl, J. L. Hewett, and T. G. Rizzo. Phenomenology of the Randall-Sundrum Gauge Hierarchy Model. *Phys. Rev. Lett.*, 84:2080, 2000.

[43] Michael Forger and Hartmann Romer. Currents and the energy momentum tensor in classical field theory: A Fresh look at an old problem. *Annals Phys.*, 309:306–389, 2004.

[44] Lisa Randall and Raman Sundrum. Large mass hierarchy from a small extra dimension. *Phys. Rev. Lett.*, 83:3370–3373, Oct 1999.

[45] Chuan-Ren Chen and Ian Low. Double take on new physics in double Higgs boson production. *Phys. Rev.*, D90(1):013018, 2014.

[46] Roberto Contino, Margherita Ghezzi, Mauro Moretti, Giuliano Panico, Fulvio Piccinini, and Andrea Wulzer. Anomalous Couplings in Double Higgs Production. *JHEP*, 08:154, 2012.

[47]

[48] J. Alwall, R. Frederix, S. Frixione, V. Hirschi, F. Maltoni, O. Mattelaer, H. S. Shao, T. Stelzer, P. Torrielli, and M. Zaro. The automated computation of tree-level and next-to-leading order differential cross sections, and their matching to parton shower simulations. *JHEP*, 07:079, 2014.

[49] Thomas Junk. Confidence level computation for combining searches with small statistics. *Nucl.Instrum.Meth.*, A434:435, 1999.

[50] Glen Cowan, Kyle Cranmer, Eilam Gross, and Ofer Vitells. Asymptotic formulae for likelihood-based tests of new physics. *Eur. Phys. J.*, C71:1554, 2011. [Erratum: Eur. Phys. J.C73,2501(2013)].

[51] SM Higgs Combination. Technical Report CMS-PAS-HIG-11-011, CERN, Geneva, 2011.

[52] S. Frixione, P. Nason, and C. Oleari. Matching nlo qcd computations with parton shower simulations: the powheg method. *JHEP*, 11:070, 2007.

[53] S. Agostinelli et al. GEANT4—a simulation toolkit. *Nucl. Instrum. Meth. A*, 506:250, 2003.

[54] Gionata Luisoni, Paolo Nason, Carlo Oleari, and Francesco Tramontano. $HW^{\pm}$/HZ + 0 and 1 jet at NLO with the POWHEG BOX interfaced to GoSam and their merging within MiNLO. *JHEP*, 10:083, 2013.

[55] Comparison of nuisances for background only case, 350 GeV mass hypothesis. http://rkamalie.web.cern.ch/rkamalie/feb12/Comparison_of_nuisances_expectedSignal0_3

[56] Comparison of nuisances for s+b case, 350 GeV mass hypothesis. http://rkamalie.web.cern.ch/rkamalie/feb12/Comparison_of_nuisances_expectedSignal1_3

[57] k-factor for DY/Z. https://twiki.cern.ch/twiki/bin/viewauth/CMS/SummaryTable1G25ns#D

[58] The LHC Higgs cross-section working group. https://twiki.cern.ch/twiki/bin/view/LHCPhysics/LHCHXSWG.

[59] Standard Model Cross Sections for CMS at 13 TeV. https://twiki.cern.ch/twiki/bin/viewauth/CMS/StandardModelCrossSectionsat13TeVInclusi

[60] SM Higgs production cross sections at sqrt(s) = 13 TeV. https://twiki.cern.ch/twiki/bin/view/LHCPhysics/CERNYellowReportPageAt13TeV#ZHllH

[61] NNLO+NNLL top-quark-pair cross sections. https://twiki.cern.ch/twiki/bin/view/LHCPhysics/TtbarNNLO#Top_quark_pair_cross_se

[62] Single Top Cross sections. https://twiki.cern.ch/twiki/bin/viewauth/CMS/SingleTopSigma.

[63] CMS GEN XSEC Task Force. https://twiki.cern.ch/twiki/bin/viewauth/CMS/GenXsecTaskF

[64] SM Higgs Branching Ratios and Total Decay Widths (update in CERN Report4 2016). https://twiki.cern.ch/twiki/bin/view/LHCPhysics/CERNYellowReportPageBR#Higgs_2_g

[65] Ryan Gavin, Ye Li, Frank Petriello, and Seth Quackenbush. W Physics at the LHC with FEWZ 2.1. *Comput. Phys. Commun.*, 184:208, 2013.

[66] Stefano Frixione, Paolo Nason, and Giovanni Ridolfi. A Positive-weight next-to-leading-order Monte Carlo for heavy flavour hadroproduction. *JHEP*, 09:126, 2007.

[67] J. Alwall, R. Frederix, S. Frixione, V. Hirschi, F. Maltoni, O. Mattelaer, H. S. Shao, T. Stelzer, P. Torrielli, and M. Zaro. The automated computation of tree-level and next-to-leading order differential cross sections, and their matching to parton shower simulations. *JHEP*, 07:079, 2014.

[68] Gunter Zech. Upper Limits in Experiments with Background Or Measurement Errors. *Nucl. Instrum. Meth.*, A277:608, 1989.

[69] A. L. Read. Presentation of search results: the CLs technique. *J. Phys. G: Nucl. Part. Phys.*, 28, 2002.

[70] Rikkert Frederix, Emanuele Re, and Paolo Torrielli. Single-top t-channel hadroproduction in the four-flavour scheme with POWHEG and aMC@NLO. *JHEP*, 09:130, 2012.

[71] Johan Alwall et al. Comparative study of various algorithms for the merging of parton showers and matrix elements in hadronic collisions. *Eur. Phys. J. C*, 53:473–500, 2008.

[72] Serguei Chatrchyan et al. Determination of jet energy calibration and transverse momentum resolution in CMS. *JINST*, 6:P11002, 2011.

[73] John M. Campbell and R. K. Ellis. MCFM for the Tevatron and the LHC. *Nucl. Phys. Proc. Suppl.*, 205-206:10, 2010.

[74] Emanuele Re. Single-top Wt-channel production matched with parton showers using the POWHEG method. *Eur. Phys. J.*, C71:1547, 2011.

[75] Gael L. Perrin, Pedro Fernandez Manteca. Muon Identification and Isolation Scale-Factors on 2016 Dataset. `https://indico.cern.ch/event/611558/contributions/2465881/attachments/1407735/2151747/TnP_06_02_2017.pdf`.

[76] CMS Muon POG. Tracking SFs on the full 2016 data. `https://twiki.cern.ch/twiki/bin/view/CMS/MuonWorkInProgressAndPagResults#Results_on_the_full_2016_data`.

[77] Gael L. Perrin. Double Muon trigger efficiency per-leg approach. https://indico.cern.ch/event/636555/contributions/2577291/attachments/1453162/2241537/TnP_DoubleMuSF_03_05_17.pdf.

[78] Grace Dupuis. Collider Constraints and Prospects of a Scalar Singlet Extension to Higgs Portal Dark Matter. *JHEP*, 07:008, 2016.

[79] Oleg Antipin, David Atwood, and Amarjit Soni. Search for RS gravitons via W(L)W(L) decays. *Phys. Lett.*, B666:155–161, 2008.

[80] A. Liam Fitzpatrick, Jared Kaplan, Lisa Randall, and Lian-Tao Wang. Searching for the Kaluza-Klein Graviton in Bulk RS Models. *JHEP*, 09:013, 2007.

[81] Kaustubh Agashe, Hooman Davoudiasl, Gilad Perez, and Amarjit Soni. Warped Gravitons at the LHC and Beyond. *Phys. Rev.*, D76:036006, 2007.

[82] CMS Higgs PAG. List of question for the preapproval checks. https://twiki.cern.ch/twiki/bin/viewauth/CMS/HiggsWG/HiggsPAGPreapprovalChecks.

[83] CMS BTV POG. Supported Algorithms and Operating Points. https://twiki.cern.ch/twiki/bin/viewauth/CMS/BtagRecommendation80XReReco#Supported_Algorithms_and_Operati.

[84] Albert M Sirunyan et al. Search for resonant and nonresonant Higgs boson pair production in the bblnulnu final state in proton-proton collisions at sqrt(s) = 13 TeV. 2017.

[85] Abdus Salam and John Clive Ward. On a gauge theory of elementary interactions. *Nuovo Cim.*, 19:165–170, 1961.

[86] Steven Weinberg. A model of leptons. *Phys.Rev.Lett.*, 19:1264–1266, 1967.

[87] Albert M Sirunyan et al. Evidence for the Higgs boson decay to a bottom quark-antiquark pair. 2017.

[88] Albert M Sirunyan et al. Particle-flow reconstruction and global event description with the CMS detector. *JINST*, 12(10):P10003, 2017.

[89] Aruna Kumar Nayak. Reconstruction of physics objects in the CMS detector. *PoS*, CHARGED2012:010, 2012.

[90] Serguei Chatrchyan et al. Observation of a new boson at a mass of 125 GeV with the CMS experiment at the LHC. *Phys. Lett.*, B716:30–61, 2012.

[91] Georges Aad et al. Observation of a new particle in the search for the Standard Model Higgs boson with the ATLAS detector at the LHC. *Phys. Lett.*, B716:1–29, 2012.

[92] Giuliano Panico. Prospects for double Higgs production. *Frascati Phys. Ser.*, 61:102, 2016.

[93] I. Belotelov, I. Golutvin, D. Bourilkov, A. Lanyov, E. Rogalev, M. Savina, and S. Shmatov. Search for ADD extra dimensional gravity in di-muon channel with the CMS detector. CMS Note 2006/076, 2006.

[94] M. Aldaya, P. Arce, J. Caballero, B. de la Cruz, P. Garcia-Abia, J. M. Hernandez, M. I. Josa, and E. Ruiz. Discovery potential and search strategy for the standard model Higgs boson in the $H \to ZZ^\star \to 4\mu$ decay channel using a mass-independent analysis. CMS Note 2006/106, 2006.

[95] A. Brandt et al. Measurements of single diffraction at $\sqrt{s} = 630$ GeV: Evidence for a non-linear $\alpha(t)$ of the pomeron. *Nucl. Phys. B*, 514:3, 1998.

[96] W. Buchmüller and D. Wyler. Constraints on SU(5)-type leptoquarks. *Phys. Lett. B*, 177:377, 1986.

[97] CMS Collaboration. CMS technical design report, volume II: Physics performance. *J. Phys. G*, 34:995, 2007.

[98] CMS Collaboration. Jet performance in pp collisions at $\sqrt{s}$=7 TeV. CMS Physics Analysis Summary CMS-PAS-JME-10-003, 2010.

[99] S. Chatrchyan et al. The CMS experiment at the CERN LHC. *JINST*, 3:S08004, 2008.

[100] Particle Data Group, J. Beringer, et al. Review of Particle Physics. *Phys. Rev. D*, 86:010001, 2012.

[101] ALEPH, CDF, D0, DELPHI, L3, OPAL, SLD Collaborations, the LEP Electroweak Working Group, the Tevatron Electroweak Working Group, and the SLD Electroweak and Heavy Flavour Groups. Precision electroweak measurements and constraints on the Standard Model. 2010.

[102] I. Bertram, G. Landsberg, J. Linnemann, R. Partridge, M. Paterno, and H. B. Prosper. A recipe for the construction of confidence limits. Technical Report TM-2104, Fermilab, 2000.

[103] L. Moneta, K. Belasco, K. S. Cranmer, A. Lazzaro, D. Piparo, G. Schott, W. Verkerke, and M. Wolf. The RooStats Project. In *13^{th} International Workshop on Advanced Computing and Analysis Techniques in Physics Research (ACAT2010)*. SISSA, 2010. PoS(ACAT2010)057.

[104] Vardan Khachatryan et al. Search for the standard model Higgs boson produced through vector boson fusion and decaying to $b\bar{b}$. *Phys. Rev.*, D92(3):032008, 2015.

[105] Performance of muon identification in pp collisions at s**0.5 = 7 TeV. Technical Report CMS-PAS-MUO-10-002, CERN, Geneva, 2010.

[106] Serguei Chatrchyan et al. Performance of CMS muon reconstruction in *pp* collision events at $\sqrt{s} = 7$ TeV. *JINST*, 7:P10002, 2012.

[107] CMS COLLABORATION. Particle–flow event reconstruction in CMS and performance for jets, taus, and E_T^{miss}. CMS Physics Analysis Summary CMS-PAS-PFT-09-001, CERN, 2009.

[108] CMS COLLABORATION. Commissioning of the particle-flow event reconstruction with the first lhc collisions recorded in the cms detector. CMS Physics Analysis Summary CMS-PAS-PFT-10-001, CERN, 2010.

[109] Vardan Khachatryan et al. Performance of Electron Reconstruction and Selection with the CMS Detector in Proton-Proton Collisions at $\sqrt{s} = 8$ TeV. *JINST*, 10(06):P06005, 2015.

[110] CMS Collaboration. Search for pair production of first-generation scalar leptoquarks in pp collisions at $\sqrt{s} = 7$ TeV. Submitted to *Phys. Rev. Lett.*, 2010.

[111] CMS Collaboration. Performance of cms muon reconstruction in pp collision events at $\sqrt{s} = 7\,\text{TeV}$. Submitted to *J. Inst.*, 2012.

[112] ATLAS Collaboration. Search for the Higgs boson in the $H \rightarrow \text{WW}(*) \rightarrow \ell^+\nu\ell^-\bar{\nu}$ decay channel in pp collisions at $\sqrt{s} = 7$ TeV with the ATLAS detector. Submitted to *Phys. Rev. Lett.*, 2011.

[113] Matteo Cacciari and Gavin P. Salam. Dispelling the N^3 myth for the k_t jet-finder. *Phys. Lett. B*, 641:57, 2006.

[114] CMS Luminosity Measurements for the 2016 Data Taking Period. Technical Report CMS-PAS-LUM-17-001, CERN, Geneva, 2017.

[115] CMS Muon POG. Reference muon id, isolation and trigger efficiencies for Run-II. `https://twiki.cern.ch/twiki/bin/viewauth/CMS/MuonReferenceEffsRun2`.

[116] John M. Campbell, R. Keith Ellis, Paolo Nason, and Emanuele Re. Top-pair production and decay at NLO matched with parton showers. *JHEP*, 04:114, 2015.

[117] Ryan Gavin, Ye Li, Frank Petriello, and Seth Quackenbush. FEWZ 2.0: A code for hadronic Z production at next-to-next-to-leading order. *Comput. Phys. Commun.*, 182:2388, 2011.

[118] Ye Li and Frank Petriello. Combining QCD and electroweak corrections to dilepton production in FEWZ. *Phys. Rev. D*, 86:094034, 2012.

[119] Vardan Khachatryan et al. Event generator tunes obtained from underlying event and multiparton scattering measurements. *Eur. Phys. J. C*, 76(3):155, 2016.

[120] Torbjorn Sjostrand, Stephen Mrenna, and Peter Z. Skands. A Brief Introduction to PYTHIA 8.1. *Comput. Phys. Commun.*, 178:852–867, 2008.

[121] Rikkert Frederix and Stefano Frixione. Merging meets matching in MC@NLO. *JHEP*, 12:061, 2012.

[122] Simone Alioli, Paolo Nason, Carlo Oleari, and Emanuele Re. NLO single-top production matched with shower in POWHEG: s- and t-channel contributions. *JHEP*, 09:111, 2009. [Erratum: JHEP02,011(2010)].

[123] Michele de Gruttola, Caterina Vernieri, Pierluigi Bortignon, David Curry, Ivan Furic, Jacobo Konigsberg, Sean-Jiun Wang, Paolo Azzurri, Tommaso Boccali, Andrea Rizzi, Silvio Donato, Stephane Brunet Cooperstein , James Olsen, Christopher Palmer, Lorenzo Bianchini, Christoph Grab, Gael Ludovic Perrin, and Luca Perrozzi. Search for the Standard Model Higgs Boson Produced in Association with W and Z and Decaying to Bottom Quarks. http://cms.cern.ch/iCMS/jsp/db_notes/noteInfo.jsp?cmsnoteid=CMS%20AN-2015/168.

[124] Michele de Gruttola, Rami Kamalieddin, Ilya Kravchenko, Lesya Shchutska. Search for resonant diHiggs production with bbZZ decays with the 2b2l2nu signature using 35.9/fb data of 2016 pp collisions at the LHC. http://cms.cern.ch/iCMS/jsp/openfile.jsp?tp=draft&files=AN2017_198_v17.pdf.

[125] Chris Palmer. VHbb Electron Trigger and ID+ISO SFs for 2016 data. https://indico.cern.ch/event/604949/contributions/2543520/attachments/1439974/2216426/VHbb_TnP_SFs_egamma_april.pdf#search=vhbb%20AND%20cerntaxonomy%3A%22Indico%2FExperiments%2FCMS%20meetings%2FPH%20%2D%20Physics%2FEgamma%22.

[126] CMS JetMET group. Jet Energy Resolution. https://twiki.cern.ch/twiki/bin/viewauth/CMS/JetResolution.

[127] CMS MET group. MET Corrections and Uncertainties for Run-II. https://twiki.cern.ch/twiki/bin/viewauth/CMS/MissingETRun2Corrections.

[128] CMS MET group. MET Filter Recommendations for Run II. https://twiki.cern.ch/twiki/bin/view/CMS/MissingETOptionalFiltersRun2.

[129] CMS EGM POG. Multivariate Electron Identification for Run2. https://twiki.cern.ch/twiki/bin/viewauth/CMS/MultivariateElectronIdentificationRun2.

[130] Helge Voss, Andreas Höcker, Jörg Stelzer, and Frerik Tegenfeldt. TMVA, the toolkit for multivariate data analysis with ROOT. In *XIth International Workshop on Advanced Computing and Analysis Techniq ues in Physics Research (ACAT)*, page 40, 2007.

[131] CMS Higgs WG. Documentation of the RooStats -based statistics tools for Higgs PAG. https://twiki.cern.ch/twiki/bin/view/CMS/SWGuideHiggsAnalysisCombinedLimit.

[132] CMS Higgs WG. Binned shape analysis with the Higgs Combination Tool. https://twiki.cern.ch/twiki/bin/view/CMS/SWGuideHiggsAnalysisCombinedLimit#Binned_shape_analysis.

[133] bbbb team. Search for resonant pair production of Higgs bosons decaying to bottom quark-antiquark pairs in proton-proton collisions at 13 TeV. http://cms.cern.ch/iCMS/analysisadmin/get?analysis=HIG-17-009-pas-v5.pdf.

[134] Matteo Cacciari, Gavin P. Salam, and Gregory Soyez. The anti-k_t jet clustering algorithm. *JHEP*, 04:063, 2008.

[135] Torbjörn Sjöstrand, Stephen Mrenna, and Peter Skands. PYTHIA 6.4 physics and manual. *JHEP*, 05:026, 2006.

[136] C. Giunti and M. Laveder. Neutrino mixing. In F. Columbus and V. Krasnoholovets, editors, *Developments in Quantum Physics*. Nova Science Publishers, Inc., 2004.

[137] Savas Dimopoulos, Stuart Raby, and Frank Wilczek. Proton decay in supersymmetric models. *Physics Letters B*, 112(2):133 – 136, 1982.

[138] M. Della Negra, P. Jenni, and T. S. Virdee. Journey in the search for the higgs boson: The atlas and cms experiments at the large hadron collider. *Science*, 338(6114):1560–1568, 2012.

[139] Thomas Schörner-Sadenius. *The Large Hadron Collider: harvest of run 1.* Springer, Cham, 2015.

[140] CERN. *Large Hadron Collider in the LEP Tunnel*, Geneva, 1984. CERN.

[141] Lyndon R Evans and Philip Bryant. LHC Machine. *JINST*, 3:S08001. 164 p, 2008. This report is an abridged version of the LHC Design Report (CERN-2004-003).

[142] Karsten Eggert, K Honkavaara, and Andreas Morsch. Luminosity considerations for the LHC. Technical Report CERN-AT-94-04-DI. CERN-LHC-Note-263. LHC-NOTE-263, CERN, Geneva, Feb 1994.

[143] Oswald Gröbner. The LHC Vacuum System. (LHC-Project-Report-181. CERN-LHC-Project-Report-181):5 p, May 1998.

[144] Wolfgang Adam, R Frühwirth, Are Strandlie, and T Todor. Reconstruction of Electrons with the Gaussian-Sum Filter in the CMS Tracker at the LHC. Technical Report CMS-NOTE-2005-001, CERN, Geneva, Jan 2005.

[145] Thomas Lenzi. Development and Study of Different Muon Track Reconstruction Algorithms for the Level-1 Trigger for the CMS Muon Upgrade with GEM Detectors. Master's thesis, U. Brussels (main), 2013.

[146] Prospects for HH measurements at the HL-LHC. Technical Report CMS-PAS-FTR-18-019, CERN, Geneva, 2018.

[147] Combination of searches for Higgs boson pair production in proton-proton collisions at $\sqrt{s} = 13$ TeV. Technical Report CMS-PAS-HIG-17-030, CERN, Geneva, 2018.

[148] The CMS collaboration. Missing transverse energy performance of the cms detector. *Journal of Instrumentation*, 6(09):P09001, 2011.

[149] Search for resonant double Higgs production with $bbZZ$ decays in the $b\bar{b}\ell\ell\nu\nu$ final state. Technical Report CMS-PAS-HIG-17-032, CERN, Geneva, 2018.

[150] Werner Herr and B Muratori. Concept of luminosity. 2006.

[151] Charles W. Misner, K. S. Thorne, and J. A. Wheeler. *Gravitation*. W. H. Freeman, San Francisco, 1973.

[152] Cecile Noels. Literature in focus - The Large Hadron Collider: A Marvel of Technology. Literature in focus - The Large Hadron Collider: A Marvel of Technology. (BUL-NA-2009-414. 51/2009):11, Dec 2009.

[153] John Hauptman. *Particle physics experiments at high energy colliders*. 2011.

[154] CMS Collaboration. The Phase-2 Upgrade of the CMS Tracker. Technical Report CERN-LHCC-2017-009. CMS-TDR-014, CERN, Geneva, Jun 2017.

[155] Philippe Bloch, Robert Brown, Paul Lecoq, and Hans Rykaczewski. *Changes to CMS ECAL electronics: addendum to the Technical Design Report*. Technical Design Report CMS. CERN, Geneva, 2002.

[156] *The CMS hadron calorimeter project: Technical Design Report*. Technical Design Report CMS. CERN, Geneva, 1997.

[157] G Baiatian, Albert M Sirunyan, Virgil E Emeliantchik, Igor Barnes, Alvin T Laasanen, and Arnold Pompos. Design, Performance, and Calibration of CMS Hadron-Barrel Calorimeter Wedges. Technical Report CMS-NOTE-2006-138. 1, CERN, Geneva, May 2007.

[158] G L Bayatian, S Chatrchyan, H Hmayakyan, A Poblaguev, M E Zeller, and B S Yuldashev. *CMS Physics: Technical Design Report Volume 1: Detector Performance and Software*. Technical Design Report CMS. CERN, Geneva, 2006. There is an error on cover due to a technical problem for some items.

[159] CMS Collaboration. The Phase-2 Upgrade of the CMS Muon Detectors. Technical Report CERN-LHCC-2017-012. CMS-TDR-016, CERN, Geneva, Sep 2017. This is the final version, approved by the LHCC.

[160] G. Bauer et al. The CMS data acquisition system software. *J. Phys. Conf. Ser.*, 219:022011, 2010.

[161] Vardan Khachatryan et al. The CMS trigger system. *JINST*, 12(01):P01020, 2017.